

# Li<sup>+</sup>-ligand binding energies and the effect of ligand fluorination on the binding energies

Charles W. Bauschlicher, Jr.\*

*NASA Ames Research Center, Moffett Field, CA 94035*

## Abstract

The Li<sup>+</sup>-ligand binding energies are computed for seven ligands and their perfluoro analogs using Density Functional Theory. The bonding is mostly electrostatic in origin. Thus the size of the binding energy tends to correlate with the ligand dipole moment, however, the charge-induced dipole contribution can be sufficiently large to affect the dipole-binding energy correlation. The perfluoro species are significantly less strongly bound than their parents, because the electron withdrawing power of the fluorine reduces the ligand dipole moment.

Keywords: DFT binding energies

---

\* Mail Stop 230-3, Thermal Protection Materials Branch, Charles.W.Bauschlicher@nasa.gov

## I. INTRODUCTION

In lithium batteries,  $\text{Li}^+$  cations migrate through the electrolyte between the anode and cathode during discharge and charge. The desire to increase the power of batteries is putting increasing demands on the electrolyte. For example lithium metal anodes and new chemistries, such as lithium-air, depend on finding new electrolytes that will not decompose during battery operation, see for example reference 1. Increasing the electrolyte stability, without degrading the solubility of the Li salt, may be the most important step in making lithium-air batteries a reality.

Experience has shown (see for example reference 2) that the formation of a solid-electrolyte interphase (SEI) can protect the electrolyte from the highly reactive Li metal. However for lithium-air batteries, no electrolyte has been found that is completely stable for the reactive species at the cathode. The work to date suggests<sup>3,4</sup> that the abstraction of H or  $\text{H}^+$  is responsible for the electrolyte decomposition. It has been shown<sup>5</sup> that replacing the hydrogen atoms in 1,2-dimethoxyethane (DME) with methyl groups changes some of the chemistry that is occurring, showing a possible stabilization of the electrolyte. We have speculated that replacing the H atoms with F atoms might block the H and  $\text{H}^+$  loss mechanisms, and hence be another way to stabilize the electrolyte.

In this manuscript we report on computed  $\text{Li}^+$ -ligand binding energies for some typical and possible electrolytes and their perfluoro versions. Many of the non-perfluoro species have been studied previously<sup>6-13</sup> using experiment and/or theory. Many different levels of theory were used in this previous work, and while many of these calculations are expected to be quiet accurate, we are interested in applying a consistent approach to a variety of ligands in order to observe trends. While our level of theory is not the most accurate in all cases, our values are in good agreement with this earlier work. Thus our approach is expected to be sufficiently accurate for our purposes. We should also note that the bonding of one  $\text{Li}^+$  with one ligand was studied in much of the previous work, whereas we consider more than one ligand in all cases.

We are also interested in seeing if one can find a perfluoro compound that has

a  $\text{Li}^+$  binding energy similar to typical electrolytes, and therefore should be able to dissolve the lithium salt and hence be a suitable electrolyte. One expects the leading term in the  $\text{Li}^+$ -ligand binding energies will be charge-dipole and therefore it is interesting to see if the computed binding energy can be correlated with the ligand dipole moment. The  $\text{Li}^+$  will have a full shell of electrolyte molecules in a battery, therefore we consider the systems with from one to the maximum number of ligands to gain insight into the bonding and how it changes with the number of ligands. This insight could help design better molecules for use as a battery electrolyte.

## II. METHODS

The  $\text{Li}^+$ -ligand binding energies are computed using Density Functional Theory (DFT). The B3LYP<sup>14</sup> hybrid<sup>15</sup> functional is used. Most calculations are performed using the 6-31+G\*\* basis of Pople and coworkers<sup>16</sup>. The accuracy of this basis set is confirmed in a few calibration calculations using the augmented correlation consistent polarized valence triple zeta (aug-cc-pVTZ) basis sets developed by Dunning and coworkers<sup>17,18</sup>. The geometries are fully optimized and the harmonic frequencies computed. The harmonic frequencies confirm that the structures correspond to minima and are used (unscaled) to compute the zero-point energies.

All of the DFT calculations are performed using Gaussian 09<sup>19</sup>, while Jmol<sup>20</sup> is used to view the structures. We use an ultrafine grid and  $10^{-11}$  integral accuracy (i.e. int=(acc2e=11,grid=ultrafinegrid)) for all calculations, except for the acetonitrile calculations where the rotation of the  $\text{CH}_3$  group leads to numerical problems. For these species, the tight optimization threshold and the superfinegrid options are used.

## III. RESULTS AND DISCUSSION

The parent ligands studied include acetonitrile (ACN), benzene ( $\text{C}_6\text{H}_6$ ), hexamethylphosphoramide (HMPA), tetrahydrofuran (THF), pyridine, 1,2-dimethoxyethane (DME), and a methyl substituted version of DME (MeDME),

where the four H atoms on the central  $C_2$  are replaced with methyl groups. In addition, we consider the perfluoro versions of these species. **The binding energies are given in Table I along with previous work<sup>7-13</sup>, and overall the current work is in good agreement pervious theory and experiment. The Li-ligand bond distances are give in Table II.**

The  $Li^+(ACN)_n$  species are shown in Fig. 1. In  $Li^+ACN$ , the N points at the  $Li^+$  and the Li-N-C atoms are on a line, thus yielding  $C_{3v}$  symmetry. For  $Li^+(ACN)_2$  the heavy atoms are on a line and the H atoms are staggered, yielding  $D_{3d}$  symmetry.  $Li^+(ACN)_3$  has  $C_{3h}$  symmetry, with all the heavy atoms in a plane.  $Li^+(ACN)_4$  has  $T_d$  symmetry. The heavy atoms in  $Li^+(ACN)_5$  form a trigonal bipyramid; the symmetry of the full molecule is  $C_3$ . The heavy atoms in  $Li^+(ACN)_6$  nearly have  $O_h$  symmetry, while the symmetry of the molecule is  $C_1$ . An inspection of the structures suggests that the ligands have arranged themselves around the  $Li^+$  in a manner that minimizes the ligand-ligand repulsion. Changing all of the hydrogen atoms to fluorines, does not change the overall shape of the molecules. We find that there are very small distortions for  $Li^+(ACN)_4$  and  $Li^+(ACN)_5$ , that lower the symmetry, but hardly affect the shape of the molecule; for  $Li^+(ACN)_4$  the energy lowering associated with this distortion is 0.2 kJ/mol. Thus for ACN, the normal and perfluoro version have very similar structures, but the ACN binding energies are significantly larger than those of the analogous perfluoro version, see Table I. The smaller binding energy for the perfluoro version is expected since the F withdraw electrons, thus reducing the charge on the N atom. The difference is clearly visible in the dipole moment, which decreases from 4.00 D for ACN to 1.18 D for the perfluoro version. We should note that for both sets of molecules the total binding energies increase significantly from 1 to 4 ligands, then increase much more slowly for 5 and 6 ligands. Clearly the ligand-ligand repulsion becomes sizable for the last two ligands. The similar total binding energies for 4, 5, and 6 ligands is consistent with the experimental observation<sup>6</sup> that the lithium coordination with in solution is 4, 5, and 6 ACN molecules. **The Li-ligand distances shown in Table II; the distance increases with the number of ligands and the perfluoro version has a longer bond length than its parent. That is, the Li-ligand distances are correlated with the repulsion and the total binding**

**energy.**

The pyridine ligands arrange themselves around the  $\text{Li}^+$  in a manner that minimizes ligand-ligand repulsion, analogous to the ACN case. The  $\text{Li}^+(\text{pyridine})$  is a planar system with  $C_{2v}$  symmetry with the  $\text{Li}^+$  located next to the nitrogen. In  $\text{Li}^+(\text{pyridine})_2$  the pyridines are on the opposite sides of the  $\text{Li}^+$ , with a skewed orientation, which yields  $D_{2d}$  symmetry.  $\text{Li}^+(\text{pyridine})_3$  has  $D_3$  symmetry. While the Li and nitrogen atoms in  $\text{Li}^+(\text{pyridine})_4$  have essentially  $T_d$  symmetry, the overall symmetry is  $S_4$ . The symmetries are unchanged in the analogous perfluoro systems. **The Li-N bond distances, see Table II are consistent with those found for the ACN species.** The dipole moment of pyridine is 2.38 D while that of the perfluoro analogue is 0.99 D. Not surprisingly, the perfluoro versions are less strongly bound than the analogous hydrogen version, see Table I. An inspection of the table shows that the pyridine binding energies are very similar to those of the ACN species.

The overall structure of the  $\text{Li}^+(\text{THF})_n$  species show a great similarity with the pyridine, with the  $\text{Li}^+$  being next to the oxygen in THF compared with the nitrogen in pyridine. The optimized structures are shown in Fig. 2. As for ACN and pyridine, replacing the hydrogen atoms with fluorines reduces the dipole moment from 2.01 D for THF to 0.29 D for the perfluoro version. This change in the charge distribution leads to two orientations of the  $\text{Li}^+$  with respect to the perfluoroTHF: 1) the  $\text{Li}^+$  is next to the oxygen and a fluorine atom on the adjacent carbon and 2) the  $\text{Li}^+$  is above the plane of the ring, interacting with three fluorine atoms. In Fig. 2 structures 5 and 6 show the two positions of the  $\text{Li}^+$ . **As shown in Table II, the Li-O and Li-F distances are very similar in 1) and the Li has a slightly asymmetric with respect to the three F atoms in 2).** For  $\text{Li}^+$  with one and two perfluoroTHF ligands, the above the ring is more strongly bound, 83.9 vs 71.8 kJ/mol for one ligand and 143.6 vs 129.5 kJ/mol for two ligands. Note only the above the ring structure for two ligands is shown in Fig. 2. **We note that the difference for one ligand is 12.1 kJ/mol and 14.2 kJ/mol for two ligand, which is significantly less than twice that for one ligand. This is result of the ligand-ligand repulsion.** When three and four ligands are surrounding the  $\text{Li}^+$ , the oxygen bonding becomes more favorable as it has less ligand-ligand repulsion. An inspection

of the binding energies in the table shows that while the THF values are very similar to ACN and pyridine, the perfluoro version of THF is very different from the perfluoro ACN and perfluoropyridine. We should also note that the binding energies for one ligand computed using the larger aug-cc-pVTZ basis set are in good agreement with that obtained using the smaller 6-31+G\*\* basis set, see Table I.

The  $C_6H_6$  and  $C_6F_6$  are another example of changes in structure with the substitution of fluorine for hydrogen. The most stable form of  $Li^+C_6H_6$  has the  $Li^+$  above the ring, while the most stable form of  $Li^+C_6F_6$  has the  $Li^+$  two-fold bonding to  $C_6F_6$ , compare structures 1 and 4 in Fig. 3. As shown in Table I, the  $Li^+$  above the  $C_6F_6$  ring has a weakly bound minima, while we were unable to find a stable planar  $Li^+C_6H_6$  structure. We note that the binding energy for  $C_6F_6$  is similar in both the 6-31+G\*\* and aug-cc-pVTZ basis sets, see Table I. The second ligand for  $C_6H_6$  and  $C_6F_6$  adopt the same orientation as the first, with a binding energy similar to the first, compare structures 2 and 5 in Fig. 3. The addition of a third  $C_6H_6$  did not result in a structure with three ligands interaction with the  $Li^+$ . Due to the large ligand-ligand repulsion, the system rearranged into two ligands bound to the  $Li^+$ , with third ligand in a second shell, see structure 3 in Fig. 3. Since the third  $C_6H_6$  hardly interacts with the  $Li^+$ , it is very weakly bound as shown in the table. For  $C_6F_6$  the two-fold binding allows three ligands to bind to the  $Li^+$  (see Fig. 3) and therefore, the binding energy for three ligands is 41.2 kJ/mol larger than for two ligands, compared with the 9.2 kJ/mol for the analogous  $C_6H_6$  structures. **For  $Li^+(C_6F_6)_4$  the molecule does not have a tetrahedral structure, see the two orientations in Fig. 3 structure 7. Two ligands have two-fold bonding while the other two have one F interacting with the Li atom. The Li atom and the 6 F atoms interacting with it have nearly  $D_{2h}$  symmetry.** The large ligand-ligand repulsion for the four  $C_6F_6$  ligands results in the change in structure compared to the other species and the very small increase in binding energy between three and four ligands for this case.

The binding of  $Li^+$  to one HMPA is significantly stronger than for the other ligands. The binding is at the oxygen site as expected. The large binding energy is consistent with the ligand dipole moment of 4.41 D. The perfluoroHMPA has a

dipole moment of 1.71 D, which indicates that substituting fluorine atoms for the hydrogens in HMPA, redistributes the charge as found for the other system, but still leaves this molecule with a sizable dipole moment and significant bonding. In fact the first ligand binding energy for perfluoroHMPA is about the same size as ACN and pyridiene. **For HMPA, the Li, O, and P atoms lie on a line. In the perfluoro analogue, the fluorine atoms results in the Li atom not sitting on the P-O axis as for Li<sup>+</sup>HMPA, but rather shifted toward a pair of the F atoms, see Fig. 4 and the bond lengths in Table II. We tried several structures where the Li interacted with only F atoms, but these species were at least 74 kJ/mol less strongly bound.** The second ligand adds to the opposite side of the first ligand, thus minimizing the ligand-ligand repulsion and the binding energies of HMPA and perfluoroHMPA are still larger than for the other systems. **For HMPA, the Li, O, and P atoms still lie on a line, while the perfluoro species has the Li interacting with both the F and O atoms, as found for one HMPA. However, ligand-ligand repulsion causes the ligand to rotate so that the Li interacts with the oxygens and only one F per ligand, not two as in one ligand case. The structures with Li interacting with three F atoms on both ligands are at least 150 kJ/mol less strongly bound.** For HMPA the difference between the first and second ligand binding is larger than for ACN, while for the perfluoroHMPA the value is **is between the values for ACN and its perfluoro analogue.** For three ligands, the Li and oxygen atoms have  $D_{3h}$  symmetry, but we should note that the ligands are canted so that the Li, oxygen, and phosphorous atoms have  $C_3$  symmetry. **An inspection of Fig. 4 shows that canting is caused by hydrogen bonding between the H atoms of one ligand with the O atom of its neighbor. In the perfluoro species, the Li-O-P angle is still not 180°, but the ligand-ligand repulsion has resulted in F atom tilting away from the Li, so that now the Li-F distances are all longer the 3 Å.** Thus three ligand are arranged to minimize repulsion. The difference between the second and third HMPA binding energies for both HMPA and perfluoroHMPA are now very similar to those found for ACN. When the fourth HMPA is added, the HMPA system has the expected  $T_d$  like arrangement, while the

perfluoroHMPA adopts a 3+1 configuration, where the fourth ligand goes into the second coordination shell. Thus the larger ligand-ligand repulsion for the perfluoro system results in a different structure. **We should note that the  $\text{Li}^+(\text{HMPA})_4$  distorts to allow hydrogen bonding between the ligands as found for the three perfluoro ligand case.**

The  $\text{Li}^+$  binding with DME and MeDME is two-fold through the oxygen atoms. That is, the oxygens are cis in the complex, while the most stable configuration of free DME has the oxygens trans. We compute the difference between cis and trans conformations of DME(MeDME) to be 1.8(10.8) kJ/mol. For perfluoroDME we find the cis to be lower than the trans by 0.5 kJ/mol. We compute the  $\text{Li}^+$  binding energy with respect to the cis conformer even though this is not the lowest for DME and MeDME. **In addition to the two-fold oxygen bonding, two other configurations were tried for the perfluoroDME. The Li interacting with one O and one F atom and interacting with two F atoms; these were found to be 3.9 and 14.8 kJ/mol higher in energy than the two-fold oxygen bonding, respectively.** The binding energies in Table I show that replacing the central H atoms with methyl groups increases the binding energy slightly. It is interesting that the dipole moment for DME (1.49 D) is larger than that of MeDME (0.91 D), despite the smaller binding energy. However, the polarizability of MeDME ( $114.3 a_0^3$ ) is about twice that of DME ( $65.3 a_0^3$ ) suggesting that the charge induced dipole contribution to the bonding leads to a larger MeDME binding energy, despite its smaller dipole moment. Since the fluorines withdraw charge, it is not surprising that dipole moments of the perfluoro version are smaller than for the parents -0.18 and 0.49 D for the perfluoroDME and perfluoroMeDME, respectively. Since the polarizabilities of the two perfluoro compounds are very similar, the binding energies follow the order expected based on the dipole moments. As expected the, the binding energies for the perfluoro compounds are much smaller than those of the parents.

## IV. CONCLUSIONS

The  $\text{Li}^+(\text{ligand})_n$  binding were computed for seven ligands and their perfluoro analogs using DFT. The bonding is electrostatic in origin, with the largest term being the charge-dipole contribution to the bonding, but the charge-induced dipole term can be sizable; for example MeDME is more strongly bonded than DME, even though DME has a larger dipole moment. The binding energies decrease with each successive ligand as a result of ligand-ligand repulsion. For those systems that have been used as electrolytes in lithium batteries, the total binding energies for the maximum number of ligands is about 100 kcal/mol or more. The binding energies for the perfluoro versions of these ligands have smaller binding energies than their parents, with only perfluoroHMPA having a total binding energy (98.3 kcal/mol) near 100 kcal/mol. The dramatic reduction in the binding energy for the perfluoro species is a result of the electron withdrawing by the fluorine atoms which significantly reduces the ligand dipole moment. The fluorine atoms also increase the size of the ligand and hence increase the ligand-ligand repulsion. We should also note that the  $\text{Li}^+$ -perfluoro species can have a different structure than the analogous hydrogen containing system.

## V. ACKNOWLEDGMENTS

This work was funded by the NASA ARMD Convergent Aeronautics Solutions (CAS) project.

---

<sup>1</sup> B.D. McCloskey, D.S. Bethune, R.M. Shelby, T. Mori, R. Scheffler, A. Speidel, M. Sherwood, A.C. Luntz, *J. Phys. Chem. Letts.* 3 (2012) 3043-3047 .

<sup>2</sup> J.B. Haskins, W.R. Bennett, J.J. Wu, D.M. Hernández, O. Borodin, J.D. Monk, C.W. Bauschlicher, J.W. Lawson, *J. Phys. Chem. B* 118 (2014) 11295-11309.

<sup>3</sup> J.M. Garcia, H.W. Horn, J.E. Rice, *J. Phys. Chem. Letts.* 6 (2015) 1795-1799.

<sup>4</sup> V. K.C. Chau, Z. Chen, H. Hu, K.-Y. Chan, *J. Electrochem. Soc.* 164 (2017) A284-A289.

- <sup>5</sup> B.D. Adams, R. Black, Z. Williams, R. Fernandes, M. Cuisinier, E.J. Berg, P. Novak, G.K. Murphy, L.F. Nazar *Adv. Energy Mater.* 5 (2015) 1400867.
- <sup>6</sup> K. Yuan, H. Bian, Y. Shen, B. Jiang, J. Li, Y. Zhang, H. Chen, J. Zheng, *J. Phys. Chem.* 118 (2014) 3689-3695.
- <sup>7</sup> D. Spångberg, K. Hermansson, *Chem. Phys.* 300 (2004) 165-176.
- <sup>8</sup> R.L. Jarek, T.D. Miles, M.L. Trester, S.C. Denson, S.K. Shin, *J. Phys. Chem. A*, 104 (2000) 2230-2237.
- <sup>9</sup> J.C. Amicangelo, P.B. Armentrout, *J. Phys. Chem. A* 104 (2000)11420-11432.
- <sup>10</sup> J.M. Vollmer, A.K. Kandalam, L. A. Curtiss, *J. Phys. Chem. A* 106 (2002) 9533-9537.
- <sup>11</sup> P.B. Armentrout, *Inter. J. Mass Spectro.* 193 (1999) 227-240
- <sup>12</sup> G.D. Smith, R.L. Jaffe, H. Partridge, *J. Phys. Chem. A* 101 (1997) 1705-1715.
- <sup>13</sup> R. Amunugama, M.T. Rogers, *Int. J. Mass Spectro.*195/1996 (2000) 439-457.
- <sup>14</sup> P.J. Stephens, F.J. Devlin, C.F. Chabalowski, M.J. Frisch, *J. Phys. Chem.* 98 (1994) 11623-11627.
- <sup>15</sup> A.D. Becke, *Chem. Phys.* 98 (1993) 5648-5652.
- <sup>16</sup> M.J. Frisch, J.A. Pople, J. S. Binkley, *J. Chem. Phys.* 80 (1984) 3265-3269 and references therein.
- <sup>17</sup> T.H. Dunning, *J. Chem. Phys.* 90 (1989it) 1007-1023.
- <sup>18</sup> R.A. Kendall, T.H. Dunning, R.J. Harrison, *J. Chem. Phys.* 96 (1992) 6796-6806.
- <sup>19</sup> M.J. Frisch, et al., *Gaussian 09*, Revision d.01, Gaussian, Inc., Pittsburgh PA, 2009.
- <sup>20</sup> Jmol: an open-source Java viewer for chemical structures in 3D. <http://www.jmol.org/>

TABLE I: Li<sup>+</sup>-ligand binding energies in kJ/mol.

Molecule	normal			perfluoro	
	D <sub>0</sub>	Δ	Previous work	D <sub>0</sub>	Δ
Li <sup>+</sup> (ACN)	185.1	185.1	175 <sup>7</sup>	119.6	119.6
Li <sup>+</sup> (ACN) <sub>2</sub>	335.6	150.5		222.0	102.3
Li <sup>+</sup> (ACN) <sub>3</sub>	427.1	91.4		289.4	67.4
Li <sup>+</sup> (ACN) <sub>4</sub>	483.7	56.6	490 <sup>7</sup>	337.4	47.9
Li <sup>+</sup> (ACN) <sub>5</sub>	491.1	7.4	538 <sup>7</sup>	352.3	14.9
Li <sup>+</sup> (ACN) <sub>6</sub>	495.8	4.8		368.5	16.2
Li <sup>+</sup> (Pyridine)	190.7	190.7	181.0±14.5 <sup>13</sup> , 179.1 <sup>13</sup>	126.6	126.6
Li <sup>+</sup> (Pyridine) <sub>2</sub>	341.7	150.9		228.8	102.2
Li <sup>+</sup> (Pyridine) <sub>3</sub>	438.1	96.4		296.2	67.4
Li <sup>+</sup> (Pyridine) <sub>4</sub>	496.7	58.6		336.2	40.0
Li <sup>+</sup> (THF) <sup>a</sup>	183.8(185.4)	183.8	185 <sup>8</sup>	83.9(90.0) <sup>b</sup>	83.9
Li <sup>+</sup> (THF) <sub>2</sub>	330.6	146.9	332 <sup>8</sup>	143.6 <sup>b</sup>	59.7
Li <sup>+</sup> (THF) <sub>3</sub>	422.0	91.3	430 <sup>8</sup>	167.8	24.1
Li <sup>+</sup> (THF) <sub>4</sub>	473.5	51.5	486 <sup>8</sup>	184.2	16.4
Li <sup>+</sup> (C <sub>6</sub> H <sub>6</sub> ) top	151.8	151.8	161.1±13.5 <sup>9</sup> , 144 <sup>10</sup>	19.3	19.3
Li <sup>+</sup> (C <sub>6</sub> H <sub>6</sub> ) 2-fold <sup>a</sup>				92.5(99.6)	92.5
Li <sup>+</sup> (C <sub>6</sub> H <sub>6</sub> ) <sub>2</sub>	242.1	90.3	264.3±17.3 <sup>9</sup> , 258 <sup>10</sup>	165.4 2-fold	73.0
Li <sup>+</sup> (C <sub>6</sub> H <sub>6</sub> ) <sub>3</sub>	251.4 2+1	9.2		206.6 2-fold	41.2
Li <sup>+</sup> (C <sub>6</sub> H <sub>6</sub> ) <sub>4</sub>				218.9 mixed <sup>c</sup>	12.2
Li <sup>+</sup> (HMPA)	279.9	279.9		195.8	195.8
Li <sup>+</sup> (HMPA) <sub>2</sub>	476.6	196.7		326.8	131.1
Li <sup>+</sup> (HMPA) <sub>3</sub>	565.8	89.2		381.5	54.7
Li <sup>+</sup> (HMPA) <sub>4</sub>	606.6	40.8		413.5	32.0
Li <sup>+</sup> (DME) <sup>d</sup>	263.0	263.0	241±18 <sup>11</sup> , 265 <sup>12</sup>	100.6	100.6
Li <sup>+</sup> (DME) <sub>2</sub>	426.5	163.6	380±30 <sup>11</sup>	172.5	71.8
Li <sup>+</sup> (MeDME) <sup>d</sup>	291.2	291.2		123.5	123.5
Li <sup>+</sup> (MeDME) <sub>2</sub>	460.4	169.2		174.8	51.3

<sup>a</sup> the aug-cc-pVTZ basis results are in parentheses.

<sup>b</sup> The perfluoro analogue has a different structure as described in the text. The values in the table for 1 and 2 perfluoroTHF are for Li<sup>+</sup> above ring. The 1 and 2 perfluoroTHF values for “Li-O” bonding are 71.8 and 129.5 kJ/mol, respectively.

<sup>c</sup> the mixed structure has two 2-fold and two 1-fold ligands.

<sup>d</sup> with respect to DME or MeDME with same cis conformation as in complex.

TABLE II: Li<sup>+</sup>-ligand bond lengths, in Å.

Molecule	normal		perfluoro	
	bond	$r_e$	bond	$r_e$
Li <sup>+</sup> (ACN)	Li-N	1.902	Li-N	1.951
Li <sup>+</sup> (ACN) <sub>2</sub>	Li-N	1.933	Li-N	1.973
Li <sup>+</sup> (ACN) <sub>3</sub>	Li-N	1.983	Li-N	2.012
Li <sup>+</sup> (ACN) <sub>4</sub>	Li-N	2.048	Li-N	2.063
Li <sup>+</sup> (ACN) <sub>5</sub>	Li-N	2.227(2), 2.130(3)	Li-N	2.211(2), 2.1401(3)
Li <sup>+</sup> (ACN) <sub>6</sub>	Li-N	2.239	Li-N	2.226
Li <sup>+</sup> (Pyridine)	Li-N	1.924	Li-N	1.986
Li <sup>+</sup> (Pyridine) <sub>2</sub>	Li-N	1.958	Li-N	2.013
Li <sup>+</sup> (Pyridine) <sub>3</sub>	Li-N	2.012	Li-N	2.066
Li <sup>+</sup> (Pyridine) <sub>4</sub>	Li-N	2.091	Li-N	2.170
Li <sup>+</sup> (THF)	Li-O	1.797	Li-F	1.972, 2.087, 2.119
Li <sup>+</sup> (THF)			Li-O <sup>a</sup>	2.034
			Li-F <sup>a</sup>	2.083
Li <sup>+</sup> (THF) <sub>2</sub>	Li-O	1.831	Li-F	2.013(2), 2.100(2), 2.324(2)
Li <sup>+</sup> (THF) <sub>2</sub>			Li-O <sup>a</sup>	2.053
			Li-F <sup>a</sup>	2.124
Li <sup>+</sup> (THF) <sub>3</sub>	Li-O	1.891	Li-O	2.024
Li <sup>+</sup> (THF) <sub>4</sub>	Li-O	1.967(2), 1.968(2)	Li-O	2.138(2), 2.137(2)
Li <sup>+</sup> (C <sub>6</sub> H <sub>6</sub> ) top	Li-plane	1.883	Li-plane <sup>b</sup>	2.142
Li <sup>+</sup> (C <sub>6</sub> H <sub>6</sub> ) 2-fold			Li-F	1.957
Li <sup>+</sup> (C <sub>6</sub> H <sub>6</sub> ) <sub>2</sub>	Li-plane	2.056	Li-F	1.992
Li <sup>+</sup> (C <sub>6</sub> H <sub>6</sub> ) <sub>3</sub>	Li-plane	2.046(2), 5.396	Li-F	2.092-2.100
Li <sup>+</sup> (C <sub>6</sub> H <sub>6</sub> ) <sub>4</sub>			Li-F	2.073-2.112
Li <sup>+</sup> (HMPA)	Li-O	1.699	Li-O	1.835
			Li-F	2.019, 2.167
Li <sup>+</sup> (HMPA) <sub>2</sub>	Li-O	1.756	Li-O	1.849
			Li-F	2.238
Li <sup>+</sup> (HMPA) <sub>3</sub>	Li-O	1.856	Li-O	1.904
Li <sup>+</sup> (HMPA) <sub>4</sub>	Li-O	1.953(2), 1.960(2)	Li-O	1.910, 1.915, 1.920, 5.116
Li <sup>+</sup> (DME)	Li-O	1.862	1.988	
Li <sup>+</sup> (DME) <sub>2</sub>	Li-O	1.964	Li-O	2.055
Li <sup>+</sup> (MeDME)	Li-O	1.823	Li-O	2.011
Li <sup>+</sup> (MeDME) <sub>2</sub>	Li-O	1.943	Li-O	2.426(2), 2.311(2)

<sup>a</sup> Less stable structure with Li interacting with the O and F atoms.

<sup>b</sup> The less stable structure with Li above the plane of the C<sub>6</sub>F<sub>6</sub>.

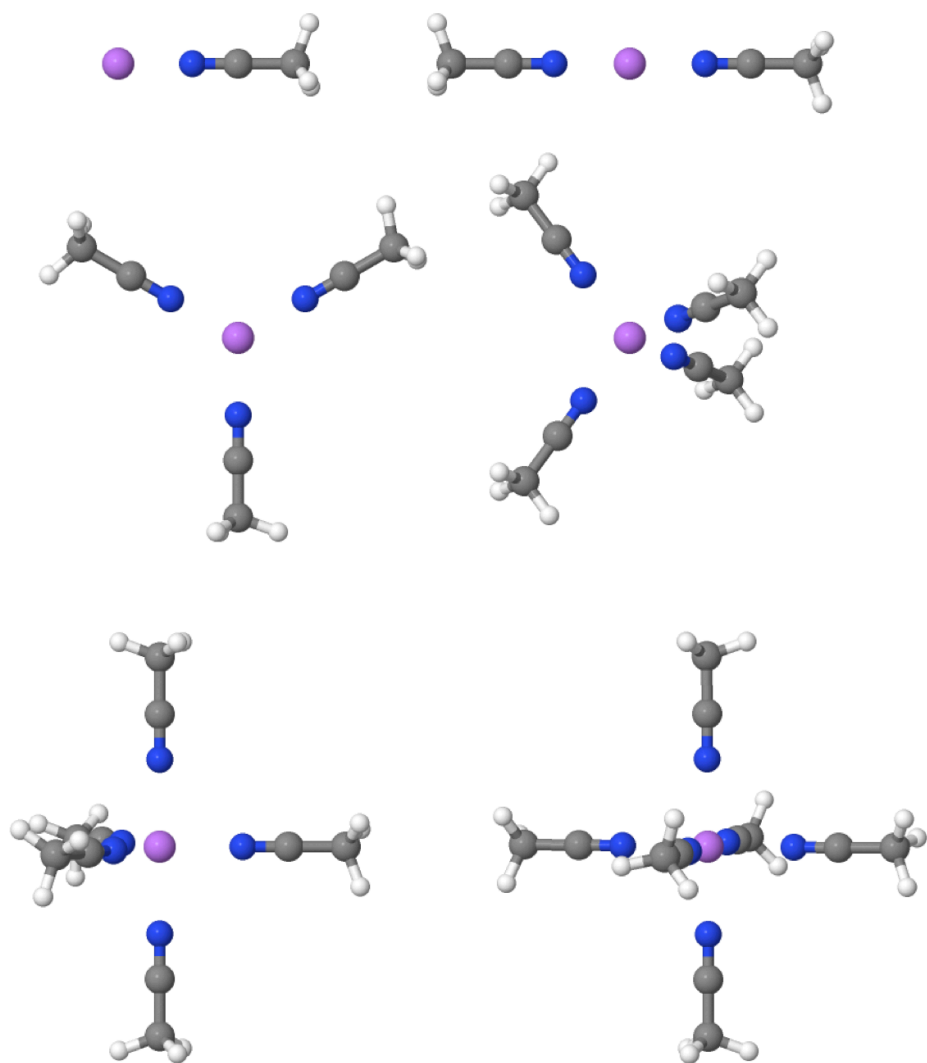


FIG. 1: The optimized structures for  $\text{Li}^+(\text{ACN})_n$ .

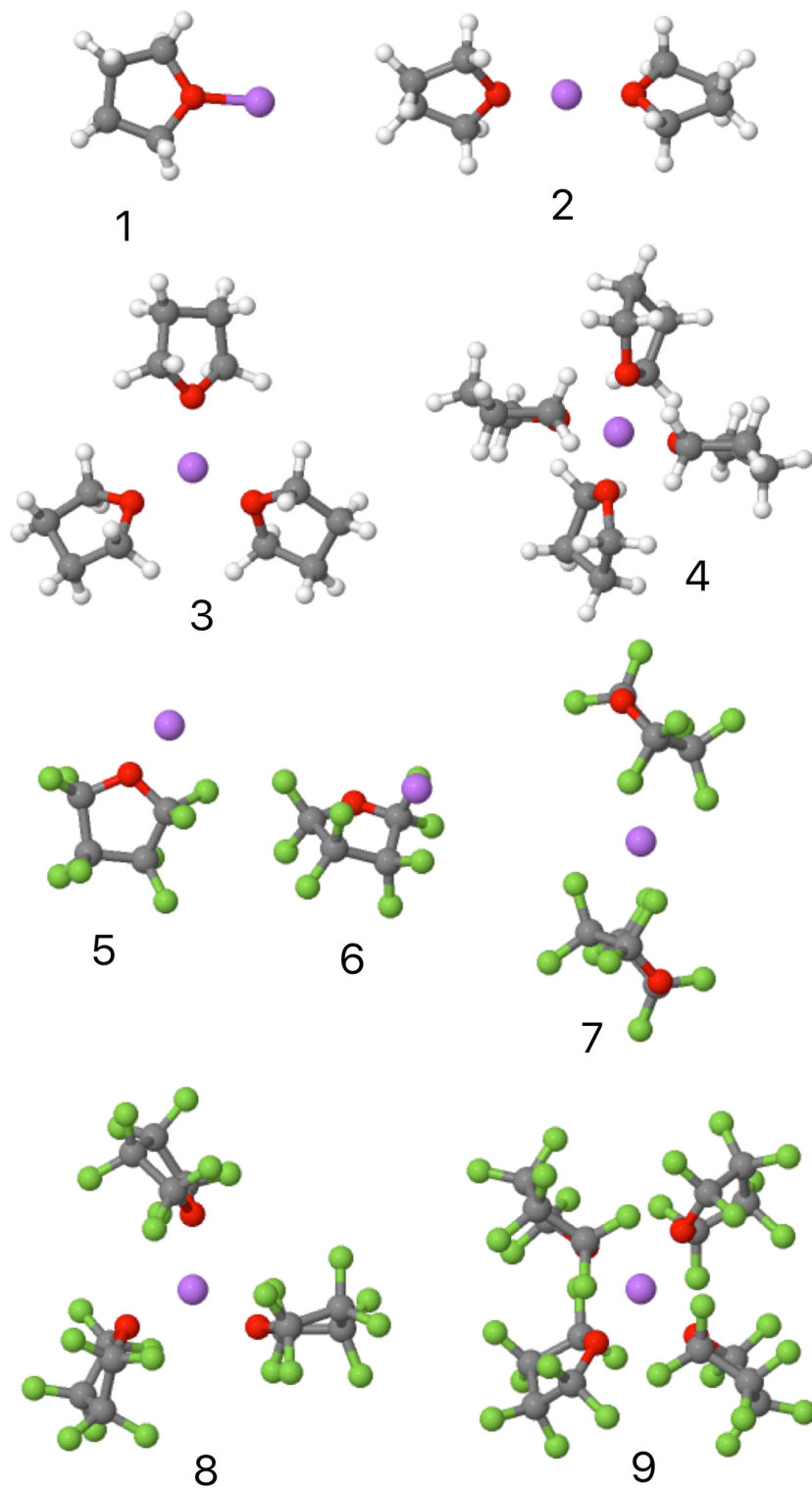


FIG. 2: The optimized structures for  $\text{Li}^+(\text{THF})_n$  and their perfluoro analogues. The structures are numbered to simplify the discussion in the text.

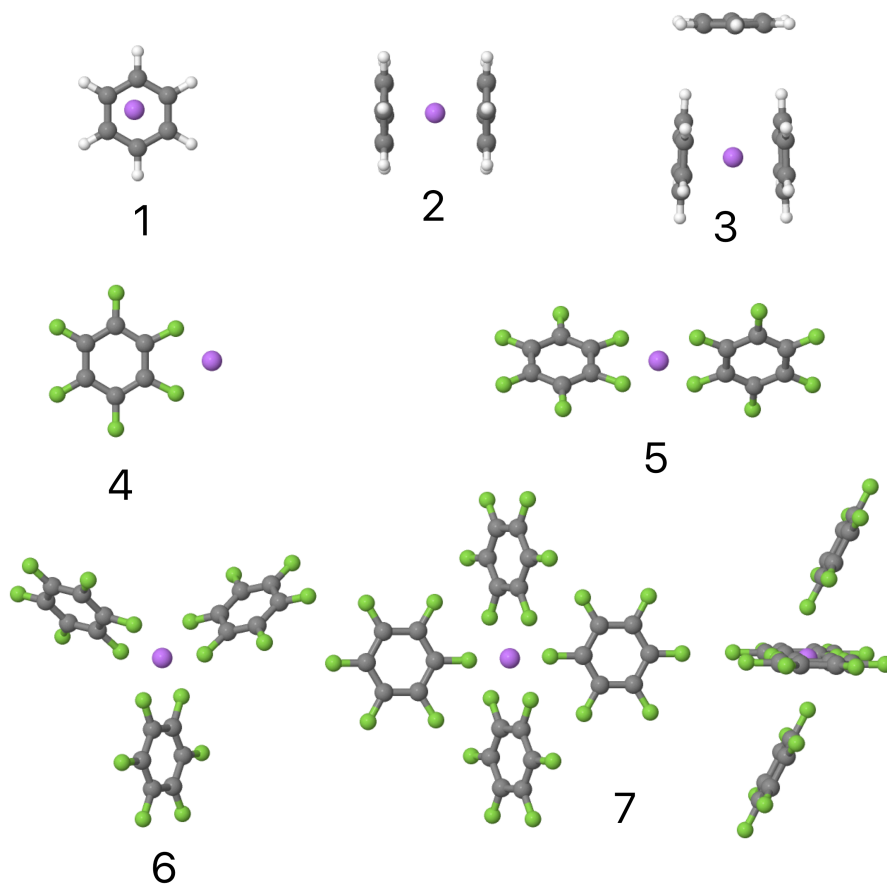


FIG. 3: The optimized structures for  $\text{Li}^+(\text{C}_6\text{H}_6)_n$  and  $\text{Li}^+(\text{C}_6\text{F}_6)_n$ . The structures are numbered to simplify the discussion in the text. Two views of the  $\text{Li}^+(\text{C}_6\text{F}_6)_4$ , structure 7, are given to better illustrate the structure.

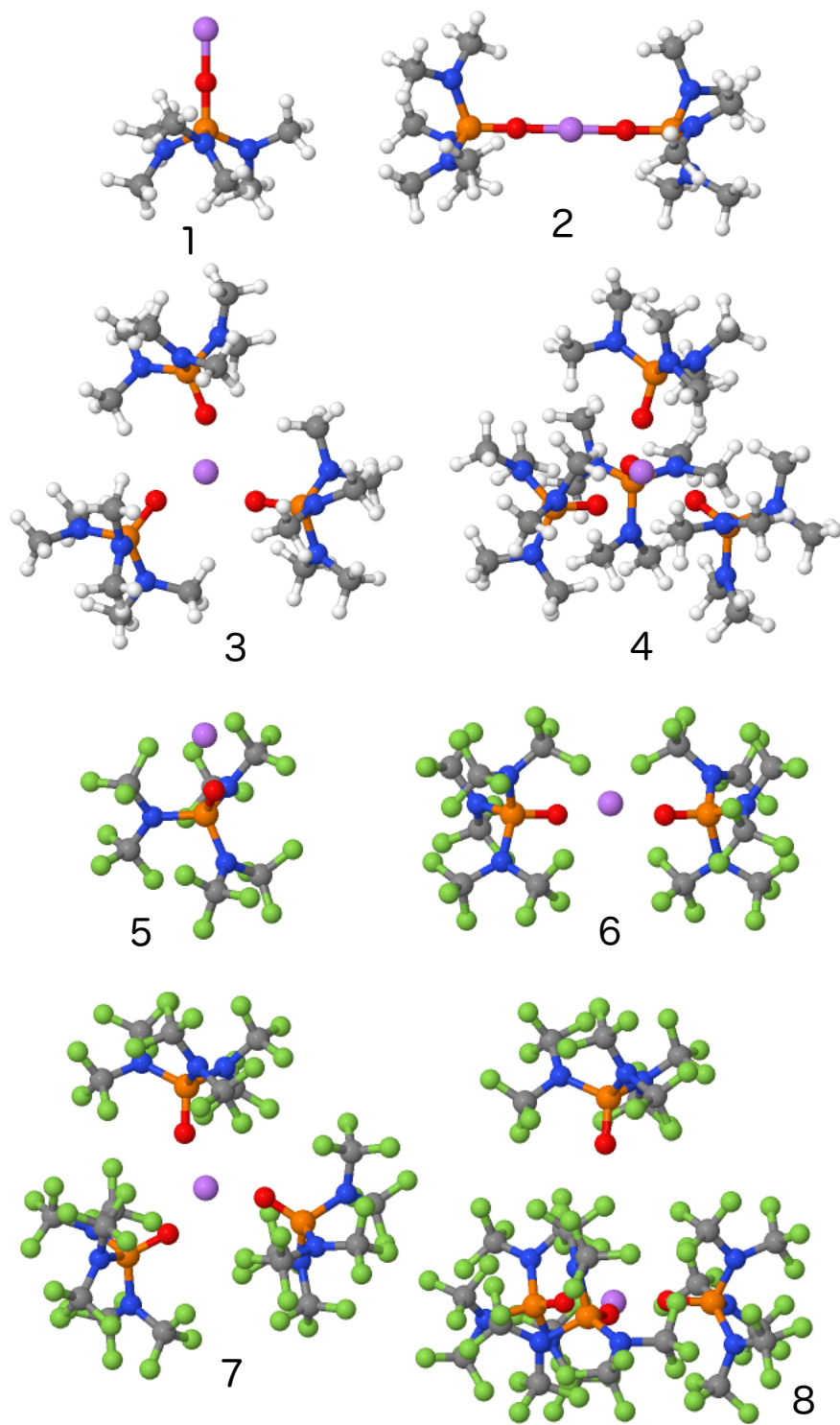


FIG. 4: The optimized structures for  $\text{Li}^+(\text{HMPA})_n$  and their perfluoro analogues. The structures are numbered to simplify the discussion in the text.